Compositional disorder and transport peculiarities in the amorphous indium oxides

U. Givan[1,2] and Z. Ovadyahu[1]
[1]*Racah Institute of Physics, The Hebrew University, Jerusalem 91904, Israel*
[2]*Max Planck Institute of Microstructure Physics, Weinberg 2, 06120 Halle, Germany*
(Received 8 July 2012; revised manuscript received 17 August 2012; published 1 October 2012)

We present results of the disorder-induced metal-insulator transition (MIT) in three-dimensional amorphous indium-oxide films. The amorphous version studied here differs from the one reported by Shahar and Ovadyahu [Phys. Rev. B **46**, 10917 (1992)] in that it has a much lower carrier concentration. As a measure of the static disorder we use the dimensionless parameter $k_F\ell$. Thermal annealing is employed as the experimental handle to tune the disorder. On the metallic side of the transition, the low temperature transport exhibits weak-localization and electron-electron correlation effects characteristic of disordered electronic systems. These include a fractional power-law conductivity versus temperature behavior anticipated to occur at the critical regime of the transition. The MIT occurs at a $k_F\ell \approx 0.3$ for both versions of the amorphous material. However, in contrast with the results obtained on the electron-rich version of this system, no sign of superconductivity is seen down to ≈0.3 K even for the most metallic sample used in the current study. This demonstrates that using $k_F\ell$ as a disorder parameter for the superconductor-insulator transition (SIT) is an ill defined procedure. A microstructural study of the films, employing high resolution chemical analysis, gives evidence for spatial fluctuations of the stoichiometry. This brings to light that, while the films are amorphous and show excellent uniformity in transport measurements of macroscopic samples, they contain compositional fluctuations that extend over mesoscopic scales. These, in turn, reflect prominent variations of carrier concentrations thus introducing an unusual type of disorder. It is argued that this *compositional* disorder may be the reason for the apparent violation of the Ioffe-Regel criterion in the two versions of the amorphous indium oxide. However, more dramatic effects due to this disorder are expected when superconductivity sets in, which are in fact consistent with the prominent transport anomalies observed in the electron-rich version of indium oxide. The relevance of compositional disorder (or other agents that are effective in spatially modulating the BCS potential) to other systems near their SIT is discussed.

DOI: 10.1103/PhysRevB.86.165101 PACS number(s): 72.80.Ng, 72.15.Rn, 68.55.Ln, 68.35.Dv

I. INTRODUCTION

The metal-insulator and the superconductor-insulator transitions (MIT and SIT respectively) are two major representatives of quantum phase transitions that have been extensively studied over the last decades. Disorder driven MIT[1] could be affected by a number of means; doping, pressure, stress, etc.[2–4] A unique method to drive the system from the insulating to the metallic (or superconducting) state is feasible in some metallic glasses prepared from the gaseous phase. Amorphous films quench-condensed onto substrates by vacuum deposition usually contain microvoids and have a lower mass density than the respective equilibrium material[5] and thus, on average, smaller interatomic overlap. Thermal treatment at precrystallization temperatures may then be used to reduce the free volume created by the microvoids.[5] In this method one controls the interatomic overlap in a similar vein as in employing hydrostatic pressure on a solid. The main difference is that thermal annealing inevitably causes an irreversible volume change.

Thermal annealing has been employed to change the resistivity of amorphous indium-oxide films while monitoring their optical properties.[6] Typically, 3–5 orders of magnitude in room temperature resistivity could be obtained accompanying a ≈3% reduction in sample thickness (measured by x-ray interferometry),[6] which is a much larger volume change than is commonly achievable by hydrostatic pressure. Using this technique, the SIT in three-dimensional indium-oxide films was mapped by measuring the low temperature conductivity as a function of disorder.[7] The amorphous indium oxide had an electron density of $\simeq 10^{21}$ cm^{-3} and the samples static disorder was characterized by $k_F\ell$ (defined in Sec. II). In this version of indium oxide, superconductivity survived in samples with $k_F\ell \gtrsim 0.24$, and, somewhat paradoxically (but reconcilable by an inhomogeneous scenario discussed in this paper), insulating behavior sets in at smaller disorder, for $k_F\ell \lesssim 0.3$. The observation that both limits are below the Ioffe-Regel criterion motivated us to conduct the present study employing the same technique of tuning disorder and using the same material but with a much smaller carrier concentration. The idea was to see whether the problem is related to the existence of superconducting or to electron-electron (*e-e)* correlations effects; in either case one expects the results to depend on carrier concentration.

In this work we map the MIT in three dimensional amorphous indium-oxide films with a carrier concentration that is 2–3 orders of magnitude lower than the material used in Ref. 7. No sign of superconductivity is found down to $T \approx 0.3$ K, and normal transport properties are observed for both the insulating and metallic regimes. However, the critical disorder, separating the metallic from the insulating regime, still appears to be given by $k_F\ell \approx 0.3$ as in the electron-rich phase. By comparison, the MIT in the previously studied[8] crystalline version of indium oxide occurs at $k_F\ell \approx 0.75$, which led us to examine the structural differences between the two phases that might account for the different $k_F\ell$ at the transition.

We present data on the microstructure of both the electron-rich and the low carrier-concentration versions of

amorphous indium oxide using high resolution microscopy and energy-dispersive local probe. Chemical analysis reveals that the indium-oxygen ratio fluctuates across the sample on mesoscopic scales. Combining this information with Rutherford backscattering and Hall effect measurements suggests that large spatial fluctuations of carrier concentration exist in these amorphous samples. The specifics of this inhomogeneity is argued to be a natural cause for a variety of transport anomalies in these as well as in other systems where superconductivity plays a role at experimentally accessible temperatures.

II. SAMPLES PREPARATION AND MEASUREMENTS TECHNIQUES

The In_xO films used here were e-gun evaporated on room-temperature microscope slides using 99.999% pure In_2O_3 sputtering target pieces. Deposition was carried out at the ambience of (2–5) $\times 10^{-4}$ Torr oxygen pressure maintained by leaking 99.9% pure O_2 through a needle valve into the vacuum chamber (base pressure $\simeq 10^{-6}$ Torr). Rates of deposition used for the samples reported here were typically 0.18–0.8 Å/s. For this range of rate-to-oxygen pressure, the In_xO samples had carrier concentration n in the range (5–13) $\times 10^{18}$ cm^{-1} measured by Hall effect at room temperature. Electron-rich In_xO samples used in the study (with carrier concentration in the 10^{21} cm^{-3} range) were produced with the conditions described earlier.[7] The films' thickness in this study was 900–1500 Å, which makes them effectively three dimensional (3D) down to the lowest temperature in our experiments ($\cong$0.3 K) for most of the samples used in this work.

The as-deposited samples had extremely high resistivity ρ of the order of 10^3–10^6 Ωcm. These were barely measurable even at room temperature. To carry out the low temperature studies, the samples ρ had to be reduced by several orders of magnitude. This was achieved by thermal annealing. A comprehensive description of the annealing process and the ensuing changes in the material microstructure are described elsewhere.[6,9] For completeness, we give here the basic protocol that was used in this study. Following deposition and initial conductance measurement, that in many cases required the use of electrometer (Keithley 617), the sample was attached to a hot stage at a constant temperature T_a, initially 5–10 degrees above room temperature. The resistance R of the sample was observed to slowly decrease over time. T_a was raised by a few degrees whenever $\Delta\rho/\rho$ over 24 hours was less than 1% (and the value of the resistance was still higher than desired). To obtain a sample with ρ that was useful for the measurements reported here usually took 20–38 thermal cycles. The annealing temperature T_a was limited to $\approx$370 K to minimize the risk of crystallization. The amorphicity of the samples during the annealing process was monitored by checking the diffraction pattern of a controlled specimen prepared on a carbon-coated copper grid. The control specimen was deposited simultaneously with the sample used for the transport measurement, but its thickness was limited to 200–300 Å to facilitate high resolution microscopy. Electron-diffraction micrograph of the as-deposited material is shown in Fig. 1(a) along with a micrograph taken for the same grid after a prolonged period of thermal annealing resulting in resistance change of more than three orders of magnitude.

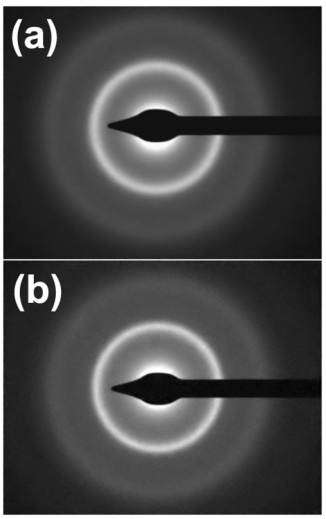

FIG. 1. Electron diffraction patterns of (a) as-prepared In_xO film and (b) the same film after thermal annealing at temperatures between 330 and 370 K for 34 days. The as-deposited sample used for transport had room-temperature two-terminal resistance larger than 120 MΩ and it dropped to 70 kΩ after annealing.

Note the characteristic broad rings of the amorphous phase, and in particular the absence of any diffraction ring of either crystalline indium oxide or metallic indium.

Conductance and Hall effect measurements were carried out on samples that were patterned in a six-probe configuration using stainless-steel masks during deposition. We used a standard Hall-bar geometry with the active channel being a strip either 0.6 mm or 1 mm wide, and 10 mm long. The two pairs of voltage probes (that doubled as Hall probes), were spaced 3 mm from one another along the strip. This arrangement allowed us to assess the large scale uniformity of the samples, both in terms of the longitudinal conductance and the Hall effect. Excellent uniformity was found on these scales; resistivities of samples separated by 1 mm along the strip were identical to within ±2% for all the samples used in the study. It should be noted however that microstructural studies performed in the course of the study revealed prominent inhomogeneities on mesoscopic scales (10^2–10^3 Å). The effects of these medium-scale irregularities on electronic transport are discussed in the next section.

Most of the conductance versus temperature $\sigma(T)$ measurements were done in the $1.3 \leqslant T \leqslant 15$ K range by a four terminal dc technique using Keithley K220 current source while monitoring the voltage with Keithley K2000. For lower temperatures measurements (down to $\approx$280 mK), we used a four terminal ac technique with the lock-in PAR124A. In all cases care was taken to maintain linear-response conditions by keeping the voltage across the sample low enough. This was verified by measuring the current-voltage characteristics at the lowest temperature of the experiment.

As in previous studies,[6–8] we use in this work $k_F\ell = (3\pi^2)^{2/3}\frac{\hbar\sigma_{RT}}{e^2 n^{1/3}}$ as a dimensionless measure of the material disorder. This is based on free-electron expressions using the measured room-temperature conductivity σ_{RT} and the carrier concentration n, obtained from Hall-effect measurements, as

input parameters. More details of preparation and characterization of In_xO samples are given elsewhere.[6]

III. RESULTS AND DISCUSSION

One of the main goals of the research was to identify the critical $k_F\ell$ at which the metal-to-insulator transition occurs in the low-n version of In_xO. This was accomplished by measuring $\sigma(T)$ over a certain range of temperatures, then extrapolating the data to $\sigma_0 \equiv \sigma\ (T \to 0)$ to determine whether the system is insulating ($\sigma_0 \leqslant 0$) or metallic ($\sigma_0 > 0$). Four different deposition batches were used in this phase of the research. In each of these, thermal annealing was used, in effect, generating samples with different $k_F\ell$ from the same physical specimen. A specific series of $\sigma(T)$ for samples labeled by their $k_F\ell$ values is shown in Fig. 2. Note that the $\sigma(T)$ plots for samples with $k_F\ell \gtrsim 0.4$ are nearly parallel to each other, a feature commonly found in many systems on the metallic side of the metal-insulator transition. The usual practice adopted in these cases is to extract the value of σ_0 by fitting the measured $\sigma(T)$ for a given sample to

$$\sigma(T) = \sigma_0 + A \cdot T^{\frac{1}{2}}, \tag{1}$$

that presumably describes transport corrections to the conductivity due to either weak-localization or e-e interactions effects.[1] Equation (1) offers a reasonably good fit to the data of samples having $k_F\ell \gtrsim 0.4$ (Fig. 2).

However, the temperature dependence of the conductance for samples that are in the immediate vicinity of the transition suggests that another $\sigma(T)$ law might be relevant, and that should perhaps be taken into account in extrapolating $\sigma(T)$ to zero temperature. So, before discussing the σ_0 versus $k_F\ell$ results we digress now to examine the data, shown in Fig. 3, for samples in the critical regime of the transition.

The figure illustrates how the form of $\sigma(T)$ changes when the system goes from metallic to insulating behavior [Fig. 3(a)]. The outstanding case is the middle curve that

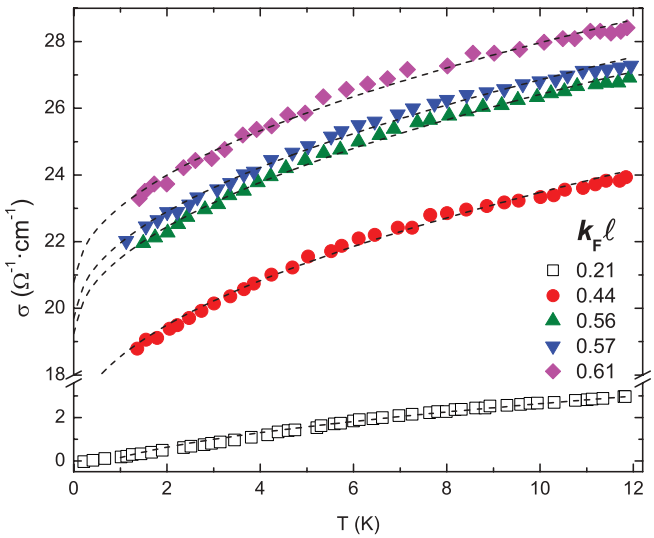

FIG. 2. (Color online) Conductivity versus temperature plots for several In_xO films labeled by their $k_F\ell$ values. Dashed lines are fits to Eq. (1) (see text).

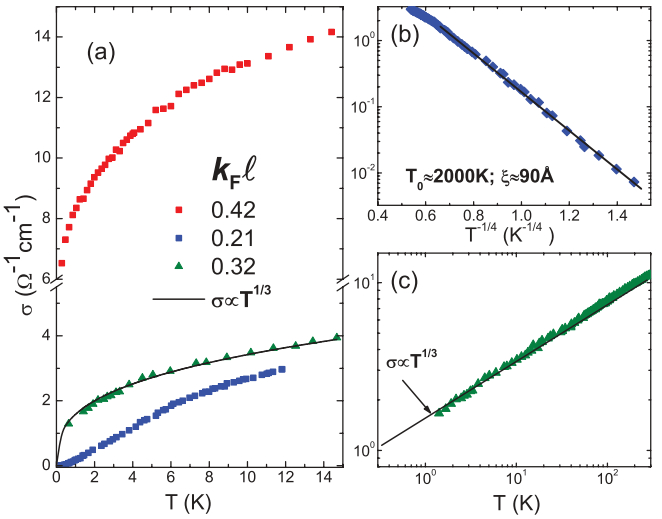

FIG. 3. (Color online) Conductivity versus temperature plots for In_xO films. (a) Samples with disorder nearest the MIT. (b) The insulating sample in (a) plotted differently to show it obeys the Mott hopping law of a three-dimensional sample; $\sigma(T) \propto \exp[-(T_M/T)^{1/4}]$. The associated localization length of this sample ξ was estimated by the Mott's formula (Ref. 5) using the experimental value for T_M. (c) Illustrating the broad temperature range over which the sample with $k_F\ell = 0.32$ (which is closest to the transition) exhibits the power-law behavior $\sigma(T) \propto T^{1/3}$.

belongs to a sample that is *just* insulating; it fits well a power-law dependence $\sigma(T) \propto T^{\frac{1}{3}}$ over a wide range of temperatures as illustrated in Fig. 3(c). A temperature dependence of this form is consistent with the interaction effect proposed by Larkin and Khmel'nitskii (LK).[10] These authors observed that at the transition the contribution of Coulomb interactions to the conductance may be expressed by

$$\sigma(T) \sim \frac{e^2 k_F}{\hbar}\left(\frac{T}{T_F}\right)^{\frac{1}{\eta}}, \tag{2}$$

where η is the exponent that describes the spatial dependence of the Coulomb potential $e\phi(r) \propto r^{-\eta}$ (with $1 < \eta < 3$). Note that this implies the lack of metallic screening at this range of disorder, heralding the approach of the dielectric phase.

An alternative to the LK mechanism, offered by Imry,[11] has been invoked to account for a $\Delta\sigma(T) \propto T^{\frac{1}{3}}$ component observed in three-dimensional In_2O_{3-x} samples near the transition.[12] The Imry mechanism takes account of the scale dependent diffusion that is a property of the critical regime. To obtain the 1/3 exponent, it also assumes a linear-with-temperature electron inelastic rate τ_{in}^{-1}. A scattering rate $\tau_{in}^{-1} \propto T$ is consistent with the results of our magneto-conductance measurements in the range 4 K $< T <$ 77 K discussed later (Fig. 9).

The conductance component associated with the Imry and the Larkin-Khmel'nitskii mechanism is proportional to $\frac{e^2}{\hbar L_{in}}$ and $\frac{e^2}{\hbar L_T}$, respectively. Here $L_{in} = \sqrt{D\tau_{in}}$ is the inelastic diffusion length (D is the diffusion constant that in the critical regime is scale dependent), and $L_T = k_F^{-1}(\frac{T}{T_F})^{\frac{1}{\eta}}$ is the LK interaction length. The prefactors associated with $\Delta\sigma$ of these

mechanisms are not presently known so we cannot determine their relative contribution. However, for either mechanism, the $T^{\frac{1}{3}}$ term should be observed once $L \ll \xi_c$ where ξ_c is the correlation length[12] and L is the relevant scale for the measurement at hand. Therefore, over some temperature range, $\sigma(T)$ of metallic samples that are sufficiently close to the transition may be describable by

$$\sigma(T) \sim \sigma_0 + A \cdot T^{\frac{1}{3}}, \tag{3}$$

where $\sigma_0 \propto \frac{e^2}{\hbar \xi_c} > 0$ and A is the sum of the contributions of the Imry and LK mechanisms.

As may be expected from the similarity between the two functions, the $\sigma(T)$ of the (metallic) samples can be fitted to either Eq. (1) or (3) almost equally well except near the transition where Eq. (3) is a better fit. For the sample with $k_F\ell = 0.42$ [top curve in Fig. 3(a)], the best fit to Eq. (3) yields a chi-square test value of $\chi^2 \simeq 0.013$ as compared with $\chi^2 \simeq 0.08$ for the best fit to Eq. (1). In general, fitting $\sigma(T)$ to Eq. (1) typically gave a higher value for the zero-temperature conductivity [the $k_F\ell = 0.42$ sample data gave $\sigma_0 \approx 6.3\ \Omega^{-1}\,\mathrm{cm}^{-1}$ versus $\sigma_0 \approx 4.1\ \Omega^{-1}\,\mathrm{cm}^{-1}$ using Eqs. (1) and (3), respectively, a ≈50% difference]. The difference in σ_0 between the two fitting possibilities however becomes less important for larger $k_F\ell$, as can be seen in Fig. 4(a). For comparison, Fig. 4(a) also includes the results of σ_0 versus $k_F\ell$ for In_2O_{3-x}, the crystalline version of 3D indium oxide.

It is noteworthy that metallic samples with $\sigma_0 \ll \sigma_{\min} = \frac{e^2}{3\pi^2\hbar} k_F$ are obtained in both systems (k_F, calculated by the free-electron expression, is $\simeq 8 \times 10^6\ \mathrm{cm}^{-1}$ and $\simeq 12 \times 10^6\ \mathrm{cm}^{-1}$ for the In_xO and In_2O_{3-x}, respectively). Quantum and *e-e* interaction effects are therefore quite prominent in the low temperature transport properties of these samples.

Data delineating the critical $k_F\ell$ for the transition in the high-n version of In_xO are shown in Fig. 4(b). This is based on the dependence of the activation energy T_0 on $k_F\ell$ for samples that are on the insulating side of the transition (but close to it).[13] These samples exhibit[7] a peculiar $\sigma(T)$ law that empirically has been fitted to simple activation: $\sigma(T) \propto \exp(-T_0/T)$. The critical $k_F\ell$ may be determined in this case by extrapolating $T_0(k_F\ell)$ to zero.[14]

Comparing the data for the three different versions of the material there are two issues that require elucidation: the difference between the various phases in terms of exhibiting superconductivity at the experimentally accessible range, and the difference in the value of $k_F\ell$ at which the metal-insulator transition occurs. Note that electron-rich In_xO samples with $k_F\ell \gtrsim 0.3$ exhibit superconductivity for $T \lesssim 3$ K [Fig. 4(b)] while the low-n In_xO version shows no sign of superconductivity down to ≈0.3 K even for samples with $k_F\ell$ as high as 0.68 (Fig. 5). It seems plausible that the difference between the high-n In_xO and the low-n version is the large disparity in their carrier concentration. Likewise, the low carrier concentration of In_2O_{3-x} ($n \approx 5 \times 10^{19}\ \mathrm{cm}^{-3}$) is presumably the main reason for the absence of superconductivity in this system.[15] A difference of 2–3 orders of magnitude in carrier concentration is large enough to push down the superconducting transition temperature T_c well below the experimental range; a mere factor of 3 in the BCS potential suffices to shift T_c from 3–4 K to less than 10 mK.

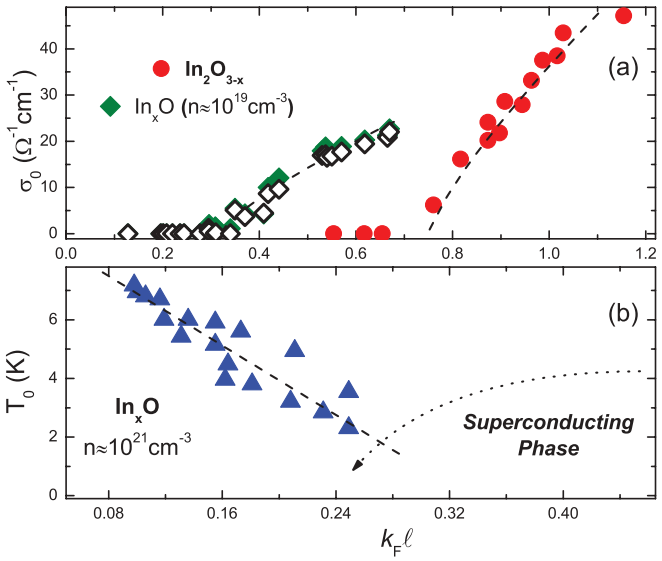

FIG. 4. (Color online) (a) The extrapolated values for the zero-temperature conductance as function of the disorder parameter $k_F\ell$. Data shown for the In_xO samples are based on extrapolation using Eq. (1) (full diamonds) and Eq. (3) (empty diamonds) respectively. The data for the crystalline version (circles) are shown for comparison (taken from Ref. 8). (b) The activation energy T_0 of electron-rich In_xO samples as function of $k_F\ell$ from which the critical disorder is estimated by extrapolation along the dashed line (see text for details). The dotted line depicts the qualitative dependence of T_c on $k_F\ell$ (based on Ref. 7).

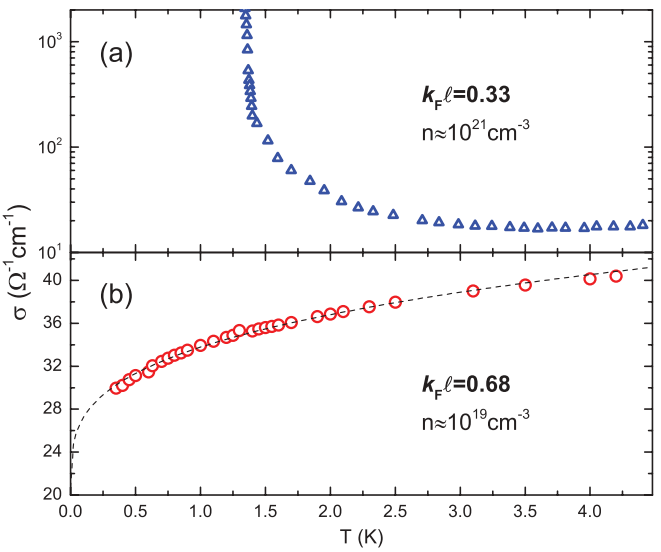

FIG. 5. (Color online) Conductivity as a function of temperature plots for two In_xO films. (a) Electron-rich sample that shows a transition to a superconducting state below $T \approx 1.5$ K (sample thickness = 1300 Å). (b) $\sigma(T)$ for In_xO sample with a much lower carrier concentration (but less disorder) exhibiting normal transport properties down to 0.3 K (sample thickness = 1000 Å). The dashed line is a fit to $\sigma(T) = \sigma_0 + A \cdot T^{0.3}$. The small value of the exponent in this case may suggest that the film is not far from crossing over to a 2D behavior at the lower temperatures (which may result in a logarithmic dependence).

The important corollary that follows from this observation is this: *$k_F\ell$ is not a good parameter to characterize disorder when superconductivity is concerned*. Reducing k_F (by e.g., decreasing the carrier concentration), weakens the BCS potential, and the superconducting transition temperature will decrease more than by reducing ℓ to achieve the same $k_F\ell$. Increasing the static disorder will reduce ℓ, but this is not necessarily detrimental to superconductivity. It may actually enhance it.[16] Even in the case that superconductivity is suppressed by disorder it is a weaker effect than the exponential decrease associated with reducing the BCS potential; the latter can easily push the transition temperature to well below experimental reach creating the false appearance of a superconductor to *metal* transition. $k_F\ell$ may still be a descriptive measure of disorder when care is taken to keep k_F constant in the process of varying the disorder as was done in Ref. 7.

Despite the huge difference in their carrier concentration (more than two orders of magnitude), the MIT in the two In_xO versions occurs at essentially the same $k_F\ell$ (see Fig. 4). Our conjecture, that the apparent violation of the Ioffe-Regel criterion in the electron-rich In_xO is due to correlations, is not supported. The low value of $k_F\ell$ at the transition is therefore more likely related to some properties of the amorphous phase that differ from the crystalline version of the material where the critical $k_F\ell$ is close to unity.

The crystalline and amorphous phases of indium oxide differ in several aspects (in addition to symmetry). While the crystalline version, in agreement with theoretical considerations,[17] behaves as a nearly free electron system,[18] optical absorption due to interband transition of In_xO samples are inconsistent with a parabolic conduction band.[6] Values of $k_F\ell$ estimated for this material by using free-electron formulas may therefore be questionable. Another possibility is that transport in the system is more inhomogeneous than might be judged by the space-filling, physically uniform structure reported for this material.[7,19,20] Note that when the sample resistivity is not uniform, $k_F\ell$ based on macroscopic measurements of conductance and carrier concentration may not be telling of the relevant disorder and the calculated value of $k_F\ell$ may differ from that associated with the "average" disorder. This could be a real problem when the inhomogeneity in the system is so gross as to cause current to flow preferentially through only part of the structure.

In the following we describe how some structural attributes of the amorphous indium oxides give rise to inhomogeneities in these systems (and possibly in other multicomponent systems like alloys and metal oxides). These may lead to a host of low temperature transport anomalies when superconductivity is involved in addition to an underestimated $k_F\ell$.

The stoichiometric compound In_2O_3 is an ionic insulator with a large ($\approx$3.6 eV) band gap. It is a well characterized material, and has a cubic structure with 48 oxygen atoms and 32 indium atoms in a unit cell. The naturally occurring material however is oxygen deficient, and films of crystalline indium oxide usually contain 5–10% oxygen vacancies.[21] This gives rise to carrier concentration $n \approx 6 \times 10^{19}$ cm^{-3}, and a factor of ± 2 around this value may be affected by changing the stoichiometry using, e.g., UV treatment.[22] The limited range of achievable n is due to constraints imposed by crystal chemistry.

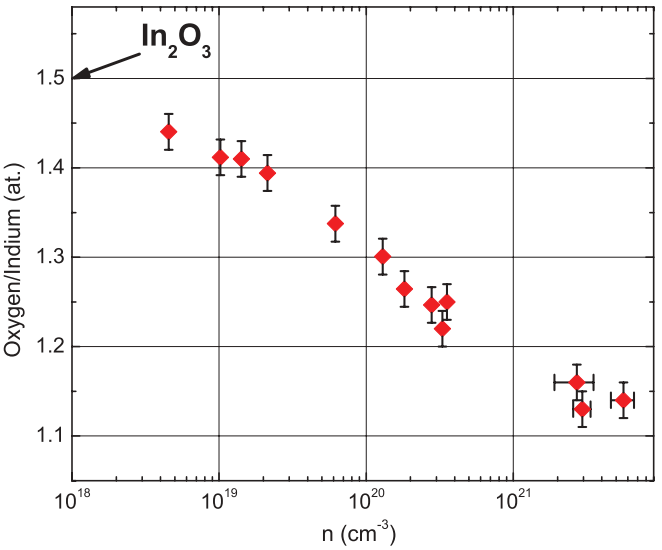

FIG. 6. (Color online) Dependence of the carrier concentration n on the In/O atomic ratio. The carrier concentration is based on room-temperature Hall effect measurements, and the O/In ratio was measured using Rutherford backscattering (see Ref. 21 for technical details).

Amorphous indium-oxide, being relatively free of these constraints, may be prepared with a much wider atomic ratio of oxygen indium. This makes it possible to make stable (more accurately, *metastable* with a long lifetime at room temperatures and below) films with optical gaps between 2.5 eV and 1.1 eV and carrier concentration of $\approx 5 \times 10^{18}$–10^{22} cm^{-3}, respectively.[6] The correlation between stoichiometry and carrier concentration of amorphous indium oxide is shown in Fig. 6.

The freedom from crystal chemistry constraints is perhaps also the reason for the emergence of *compositional*-disorder in these amorphous oxides. This kind of spatial disorder has far reaching consequences, especially when superconductivity is involved. Spatial disorder means that the material parameters vary in space; *disordered* systems are *inhomogeneous* by definition.

The nature of the inhomogeneity however, depends on the *type* of disorder. Quenched disorder of the ionic potential is common in most disordered electronic systems. Large spatial fluctuations of carrier concentration on the other hand are unlikely to occur in systems with monoatomic metallic systems, but they are quite prominent in all versions of the amorphous indium oxides. Figure 7 is a micrograph taken by a scanning mode of a transmission electron microscope. The contrast mechanism in the micrograph is due to absorption; changing the angle between the sample plane and the electron beam axis does not turn a black region into white (as it often would in a crystalline sample where the main contrast mechanism is Bragg scattering). There are no holes in the film and thickness variations are relatively small; AFM line scans show 5–20 Å surface roughness for 200 Å films deposited on glass substrates (the smaller value obtained for the low-n version of the material). Chemical analysis, using energy dispersive x-ray spectroscopy and electron energy-loss spectroscopy (EELS) revealed that regions with higher

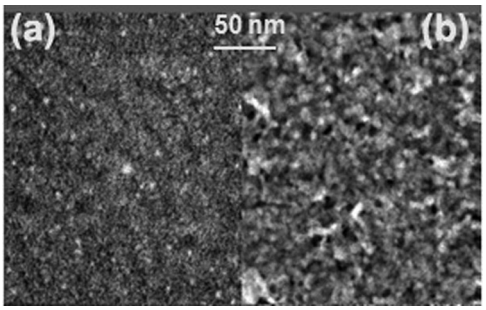

FIG. 7. STEM (scanning transmission electron microscopy) picture of In_xO films. These are typical for the low-n version with carrier- concentration $n = 5 \times 10^{18}$ cm^{-3} (a), and the electron-rich version with $n = 3 \times 10^{21}$ cm^{-3} (b). The films are 300 Å thick (rather than the 1000–1400 Å thick films used for transport) to achieve a good spatial resolution, and they were thermally annealed to make them characteristic of samples near their respective MIT (a) and SIT (b) transition.

transmission (white patches in the figure) are richer in oxygen, poorer in indium content, and vice versa for the black regions. Variations in the O-In ratio between these regions could be as high as 15–40% for a sampling area of 50 Å^2. The uncertainty in these measurements is mainly due to the background signal from the carbon support that includes a certain amount of oxygen. This source of error may be mitigated by making self-supporting films, but a systematic study of thickness dependence will be necessary to get a more accurate estimate of stoichiometry. Note, however, that a mere 10% variation in O-In ratio is equivalent to an *order of magnitude* difference in the local carrier concentration (cf., Fig. 6), which is tantamount to a factor of two in the thermodynamic density of states.

The spatial range of these compositional fluctuations can be assessed by Fourier transforming line scans of the intensity, averaged over the entire micrograph area (only a part of which is shown in Fig. 7). Results of such analyses, done for the two In_xO samples of Fig. 7, are shown in Fig. 8. The flattening out of the spectrum at the small spatial scales is partly due to the smoothing effect of oxygen diffusion and partly due to the STEM resolution. Note that the low-n In_xO is somewhat more uniform than the high-n version. However, in both cases the spectrum is skewed in a similar way and the compositional fluctuations persist over scales extending up to 300–800 Å.

These scales are comparable or even larger than the length scales that may be relevant for transport; $L_{\rm in}, L_T, \ell$, (and ξ_s, the superconducting coherence length). Pertinent information on these transport parameters may be obtained by analyzing magneto-conductance (MC) data. We have measured ten In_xO metallic samples at 4 K, and for comparison, also at 77 K. At small fields the MC for all metallic samples was positive and that remained so down to 2 K (tested on one of these samples). Spin orbit scattering in In_xO is therefore rather limited in strength. A negative MC component however does appear at high fields as seen in the data described in Fig. 9.

Figure 9 compares the MC of our most metallic In_xO sample with a In_2O_{3-x} sample of comparable resistivity. The latter system has been extensively studied and exhibits $L_{\rm in}$ of 1000–1300 Å at ≈4 K for samples with $k_F\ell$ of order 2–5.[23] The field at which the MC crosses over from H^2

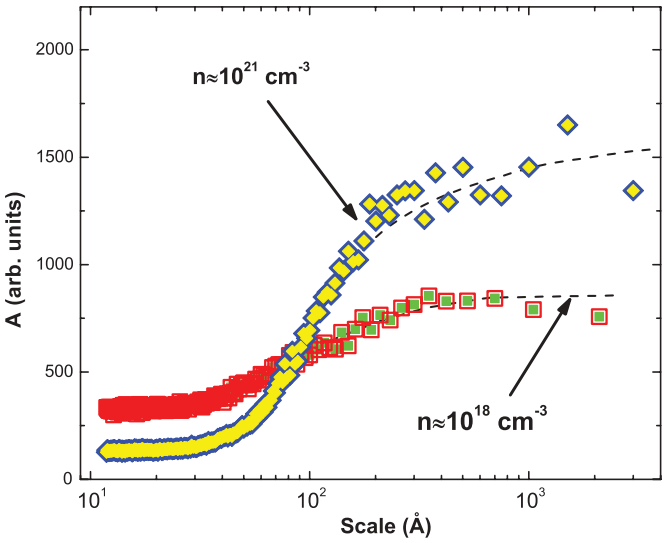

FIG. 8. (Color online) Fourier transforms of the STEM micrographs taken from the same samples shown in Fig. 7 and plotted as a function of the spatial scale. These were averaged over individual line scans taken across each micrograph. The dashed lines are merely guides to the eye.

to a weaker dependence is ≈25 times larger for the In_xO sample. This suggests a considerably smaller $L_{\rm in}$ than that of In_2O_{3-x} at the same temperature. We have analyzed the low field MC for the amorphous sample using Kawabata's[24] expression: $\frac{\Delta\sigma}{\sigma} = \frac{\tau_{el}^{1/2}\tau_{\rm in}^{3/2}e^2H^2}{12\sqrt{3}m^2}$ in conjunction with the Drude expression for the conductivity $\sigma = \frac{ne^2}{m^*}\tau_{el}$ using $m* \approx 0.28 \cdot$

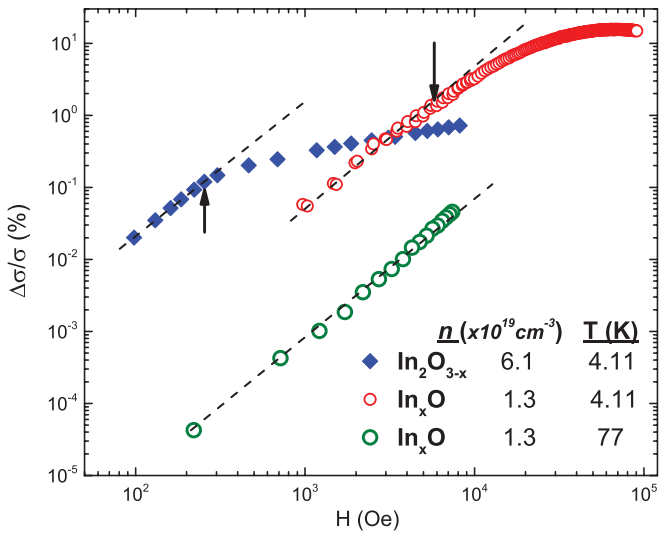

FIG. 9. (Color online) Magneto-conductance for a metallic In_xO film ($k_F\ell = 0.68$) shown for 77 K and 4.11 K. These are compared with the magneto-conductance for a crystalline indium-oxide sample (with $k_F\ell = 2.3$) taken at 4.11 K. Dashed lines depict the $\Delta\sigma/\sigma \propto H^2$ law expected for small fields. Arrows mark the fields where $\Delta\sigma/\sigma$ deviates from the parabolic law. The ratio $\Delta\sigma/\sigma$ (4 K)/$\Delta\sigma/\sigma$ (77 K) measured for ten In_xO samples in the parabolic part of the MC was 78 ± 4. Using Kawabata's expression (Ref. 24) $\Delta\sigma/\sigma \propto \tau_{\rm in}^{3/2}$; this is consistent with $\tau_{\rm in} \propto T^{-1}$ in this range of temperatures. Note the negative MC of the In_xO sample (at 4.1 K) for $H > 6.5$ T.

(mass of the free electron). This yielded the parameters: $\tau_{el} \approx 6 \times 10^{-15}$ s, $\ell \approx 12$ Å (using $V_F \approx 2 \times 10^7$ cm/s), $L_{\rm in}$ (at 4.1 K) $= 450 \pm 20$ Å, $D \approx 2$ cm^2/s. The interaction length is then 70 Å and 140 Å depending on whether $L_T = k_F^{-1}(\frac{T}{T_F})^{\frac{1}{\eta}}$ or $\sqrt{\frac{\hbar D}{k_B T}}$, respectively. At temperatures relevant for our experiments these length scales are not large enough to average out the compositional inhomogeneities observed in these materials.

Although it may have no direct bearing on the main issues of this work, it is important to point out that the MC of the In_xO samples differs from the MC in the crystalline version by more than the magnitude of $L_{\rm in}$. The negative MC component of the metallic sample in Fig. 9, that is just observable above ≈6.5 T, becomes quite noticeable at lower temperatures (but down to 1.4 K it is only seen above ≈3 T). The MC in diffusive In_2O_{3-x} samples is purely positive, throughout the entire range up to fields of 12 T and down in temperature from 77 K to ≈40 mK. There is also a difference between In_xO and the crystalline In_2O_{3-x} version in terms of the MC for insulating samples; the MC in insulating In_2O_{3-x} starts positive and becomes negative at high fields[25] while just the opposite is observed in our insulating In_xO sample (with $k_F\ell = 0.23$) for temperatures below 3 K.

Results of MC measurements on In_xO films were reported by Lee *et al*.[26] Their results differed from ours; they observed positive MC only above 8–10 K while the low field MC became negative at lower temperatures. It should be noted however that the In_xO films of Lee *et al*. were presumably the electron-rich version (and exhibited superconductivity for $T < 1$ K when the resistance was low enough). More work is needed to identify the origin of the mechanism that is responsible for the negative MC at both the metallic and insulating regime of the different versions of In_xO.

Fluctuations in carrier concentrations on the spatial scales observed in the amorphous indium oxides constitute an important type of disorder. Screening is more effective in regions with larger n, which means that the conductance in these regions is higher (although the mobility may be impaired in these regions, partially offsetting this effect). When the sample resistivity is not uniform, $k_F\ell$ based on macroscopic measurements of conductance and carrier concentration will in general be underestimated; since current naturally flows preferentially through the more conducting regions of the structure, the "active" volume for transport is smaller than that assumed by its geometric dimensions. The nonuniform current distribution affects the perceived values of both the conductivity σ and the carrier-concentration n, which are used in assigning a value of $k_F\ell$ to a given sample. This is based on $k_F\ell = (3\pi^2)^{2/3}\frac{\hbar\sigma_{\rm RT}}{e^2 n^{1/3}}$, and therefore errors in n have a lesser effect than errors in $\sigma_{\rm RT}$ unless the system inhomogeneity is excessive (the Hall voltage may be significantly suppressed in, e.g., filamentary conduction yielding a spuriously huge n). It seems intuitively plausible that, in general, inhomogeneity causes $\sigma_{\rm RT}$ to be underestimated while the Hall-derived n is if anything somewhat overestimated. These considerations may explain why the metal to insulator transition in the two versions of In_xO occurs for $k_F\ell$ that is smaller than unity. At the same time, for scales of the order of millimeters, these compositional inhomogeneities are well averaged, and therefore the excellent uniformity of the In_xO films mentioned in Sec. II is not at variance with the observed mesoscale inhomogeneity.

A more profound modification of transport should occur at low temperatures when superconductivity appears. This is where the value of $k_F\ell$ as a parameter that characterizes disorder has questionable merit; carrier-rich regions of the system are more likely to go superconducting than regions where n is small. As demonstrated in Fig. 5, the sample with the larger carrier concentration goes superconducting despite having a *smaller* $k_F\ell$ than a sample with a larger mean free path. It is the BCS potential that plays the crucial role in these situations, and when its local value fluctuates in the system on scales that are comparable or larger than ξ_s, inhomogeneity is dramatically enhanced. In this case the system breaks into a "granular-like" structure; islands of zero resistance precipitate in a normal matrix. The latter may be either metallic or insulating depending on the (average) degree of disorder, carrier concentration, and temperature. Due to proximity and Josephson effects (that are temperature dependent), the scales of the superconducting islands and their spatial distribution may somewhat differ from those set by the compositional disorder.

The following transport anomalies found in the electron-rich version of In_xO are in line with this picture:

(1) The critical disorder for the SIT is scale dependent; short samples may go superconducting while longer ones, made on the same strip and having essentially the *same* (normal state) resistivity, exhibit *insulating* behavior.[20]

(2) On the just insulating side of the transition, where the conductance versus temperature follows $\sigma(T) \propto \exp(-T_0/T)$, the activation energy T_0 increases monotonously with the sample length.[20]

(3) The current voltage characteristics of these samples revealed discontinuous jumps similar to those found in Josephson arrays.[19]

(4) A nonmonotonous MC is observable in In_xO films near their SIT; The conductance first decreases with field reaching, in some cases, a much smaller value then its asymptotic value at high fields.[27]

Significantly, all these anomalies appear at the temperature range where the less disordered material is superconducting. Other possible manifestations of superconducting islands coexisting with normal regions were obtained in Ref. 28 and in recent tunneling experiments from large area electrodes into In_xO films in the insulating regime.[29] It may be difficult to observe these nonsuperconducting regions by a scanning tunneling microscopy technique (STM) due to the spreading resistance associated with resistive paths, but the inhomogeneous nature of superconductivity has been seen by STM in In_xO films[30] (and in TiN).[31]

The observation that the In_xO films are structurally continuous, and being amorphous, free of grain boundaries etc., was an inducement to offer an inherent "disorder induced granularity" scenario for these phenomena.[19,20] The effects associated with this scenario ought to have been apparent in *all* materials near their SIT provided that superconductivity is not suppressed by disorder before a "critical G" $\approx \frac{e^2}{h}$ is reached.[19,20] Several systems such as TiN[32] and NbN[33] indeed exhibited some of these transport anomalies near their SIT (specifically, a

nonmonotonous MC). However, the magnitude of these effects were not as prominent as they are in the electron-rich In_xO samples. Moreover, these peculiarities are not usually observed near the *disorder-tuned*[34] SIT of amorphous Bi and Pb films, except when structural granularity was deliberately introduced to modify their microstructure.[35]

We have therefore to conclude that, while the "inherent disorder-induced" inhomogeneity is a plausible physical scenario, it appears that the modulation depth of local superconducting properties caused by potential fluctuations is much less conspicuous than that of fluctuations in carrier density. In other words, the *type* of disorder is an important ingredient in producing prominent "granularity effects" near the SIT. Unless they break time-reversal symmetry, potential fluctuation have a mild effect on T_c (which can be of either sign).[16] Spatial fluctuation in the BCS potential, on the other hand, is a powerful agent for local modulation of T_c, and it may facilitate the two-phase state responsible to the observed transport peculiarities. An effective way to achieve it is by modulating carrier concentration, which seem to occur naturally in the amorphous indium oxides.

This type of disorder is energetically unfavorable in a monoatomic system like amorphous Bi unless the system is physically discontinuous. On the other hand, in an alloy or metal oxide, compositional disorder may compensate for the carrier concentration difference by a chemical one without compromising the physical continuity of the structure. Grain boundaries and other extended defects may also play a role in creating inhomogeneous BCS potential distribution when pair-breakers such as magnetic impurities (that tend to segregate at these defects) are present in the system.

The corollary that emerges from these considerations is that while disorder is tantamount to inhomogeneity, the degree and detailed nature of the resulting spatial fluctuation depend on the *type* of disorder, not just on its magnitude. This distinction may be less important for the noninteracting system but it is crucial for the subtle case of superconductivity.

One of the questions raised in the study of insulating In_xO films near the SIT[7] was the origin of the dependence of the conductance on temperature $\sigma(T) \propto \exp(-T_0/T)$. An Arrhenius law for $\sigma(T)$ is intriguing in that it occurs in a disordered system for which the natural choice is the variable-range-hopping (VRH) mechanism,[5] which indeed is exhibited by just-insulating samples of the low-n version of In_xO [Fig. 3(b)]. The study reported in Ref. 7 used a three-dimensional system. The activation energy of the insulating samples increased monotonously with disorder reaching a maximum of $T_0 \approx 7$ K before the conduction mechanism reverted to variable range hopping.[7] It was shown in a subsequent study using a *two*-dimensional version of this system that T_0 may reach 14–15 K[19] for a similar range of $k_F\ell$ used in the 3D system. The dimensionality and length dependence of T_0 are characteristic signs of a percolative phenomenon.

These observations suggest that the origin of the $\sigma(T) \propto \exp(-T_0/T)$, or a somewhat *faster* dependence,[19] is the appearance of superconducting islands in an insulating medium. In the insulating regime of the SIT (and at temperatures where the material is fully in the normal state), most of the electron-rich areas are weakly coupled to other regions, say with typical coefficient $t \ll 1$. As the temperature falls below the local T_c of these regions, the coupling (being now controlled by Andreev processes), becomes $t^2 \lll 1$. Superconducting islands that were part of the current-carrying network (CCN) in the normal state, will be effectively removed from it thereby forcing a new and less conductive CCN. Transport in the VRH regime takes place in a tenuous current-carrying network that, for a given disorder, becomes more rarefied as temperature is lowered. An *exponential* reduction of the conductance occurs when part of the sample volume is eliminated from the transport,[36] a role that the superconducting islands may effectively take.

The range of disorder where this mechanism is relevant is limited to the vicinity of the transition; for sufficiently strong disorder the localization length ξ will be everywhere smaller than ξ_s and there will be no superconducting islands in the system. In this case the transport mechanism will revert to normal VRH as seen in the experiment.[7] At small disorder, on the other hand, many of the superconducting islands may be Josephson-coupled to form large superconducting clusters. Effective Josephson coupling through *insulating* In_xO layers has been observed experimentally.[37] Global superconductivity may result in the system with the associated percolative features discussed in Ref. 20. In this picture $\sigma(T)$ is a nontrivial result of hopping conductivity modulated by the compounded effect of the temperature-dependent appearance of superconducting islands *and* the evolution with temperature of their local pair potential. In view of the transport features described above this seems to be a prime avenue to look for a solution to this problem.

ACKNOWLEDGMENTS

This work greatly benefited from an extensive exchange of data and ideas with the research groups of Allen Goldman, and Aviad Frydman. We also acknowledge illuminating discussion with O. Agam, D. Khmel'nitskii, Y. Imry, and M. Feigel'man. One of us (Z.O.) expresses his gratitude to F. P. Milliken for help in getting some of the Rutherford backscattering data at the IBM research Center, Yorktown-Heights. This research has been supported by the Binational US-Israel Science Foundation and by The Israeli Academy for Sciences and Humanities.

[1] W. L. McMillan, Phys. Rev. B **24**, 2739 (1981); Patrick A. Lee and T. V. Ramakrishnan, Rev. Mod. Phys. **57**, 287 (1985).

[2] M. A. Paalanen, T. F. Rosenbaum, G. A. Thomas, and R. N. Bhatt, Phys. Rev. Lett. **48**, 1284 (1982); T. F. Rosenbaum, R. F. Milligan, M. A. Paalanen, G. A. Thomas, R. N. Bhatt, and W. Lin, Phys. Rev. B **27**, 7509 (1983).

[3] C. Sekine, T. Uchiumi, I. Shirotani, and T. Yagi, Phys. Rev. Lett. **79**, 3218 (1997).

[4] V. Laukhin, J. Fontcuberta, J. L. García-Muñoz, and X. Obradors, Phys. Rev. B **56**, R10009 (1997).

[5] N. F. Mott and A. E. Davis, *Electronic Processes in Non-Crystalline Materials* (Clarendon Press, Oxford, 1971).

[6]Z. Ovadyahu, Phys. Rev. B **47**, 6161 (1993).
[7]D. Shahar and Z. Ovadyahu, Phys. Rev. B **46**, 10917 (1992).
[8]E. Tousson, E. P. Rubenstein, R. Rosenbaum, V. Volterra, and Z. Ovadyahu, Philos. Mag. B **56**, 875 (1987); E. Tousson and Z. Ovadyahu, Phys. Rev. B **38**, 12290 (1988).
[9]Z. Ovadyahu, J. Phys. C **19**, 5187 (1986).
[10]A. I. Larkin and D. E. Khmel'nitskii, Zh. Eksp. Teor. Fiz. **83**, 1140 (1982) [Sov. Phys. JETP **56**, 647 (1982)].
[11]Y. Imry, J. Appl. Phys. **52**, 1817 (1981).
[12]Y. Imry and Z. Ovadyahu, J. Phys. C **15**, L327 (1982).
[13]Samples with $k_F\ell \gtrsim 0.25$ in this electron-rich version of In_xO are superconducting at liquid-helium temperatures, and therefore the critical $k_F\ell$ cannot be determined by the low-temperature method used for the nonsuperconducting In_2O_{3-x} and the low-n version of In_xO.
[14]M. V. Feigel'man, L. B. Ioffe, V. E. Kravtsov, and E. A. Yuzbashyan, Phys. Rev. Lett. **98**, 027001 (2007).
[15]Crystalline indium-oxide films were measured down to ≈12 mK showing no sign of superconductivity; F. P. Milliken and Z. Ovadyahu (unpublished).
[16]K. Knorr and N. Barth, Solid State Commun. **8**, 1085 (1970); E. Babić, R. Krsnik, B. Leontić, and I. Zorić, Phys. Rev. B **2**, 3580 (1970); B. Stritzker and H. Wühl, Z. Phys. B **24**, 367 (1976) and references therein; M. S. Osofsky, R. J. Soulen Jr., J. H. Claassen, G. Trotter, H. Kim, and J. S. Horwitz, Phys. Rev. Lett. **87**, 197004 (2001) and references therein.
[17]O. N. Mryasov and A. J. Freeman, Phys. Rev. B **64**, 233111 (2001).
[18]O. Cohen and Z. Ovadyahu, Phys. Rev. B **50**, 10442 (1994).
[19]D. Kowal and Z. Ovadyahu, Solid State Commun. **90**, 783 (1994).
[20]D. Kowal and Z. Ovadyahu, Physica C **468**, 322 (2008).
[21]Z. Ovadyahu, B. Ovryn, and H. W. Kraner, J. Elect. Chem. Soc. **130**, 917 (1983).
[22]Z. Ovadyahu, J. Phys. C **19**, 5187 (1986).
[23]Z. Ovadyahu, Y. Gefen, and Y. Imry, Phys. Rev. B **32**, 781 (1985) and references therein.
[24]A. Kawabata, Solid State Commun. **34**, 431 (1980).
[25]A. Vaknin, A. Frydman, Z. Ovadyahu, and M. Pollak, Phys. Rev. B **54**, 13604 (1996).
[26]Y. J. Lee, Y. S. Kim, and H. K. Shin, J. Phys.: Condens. Matter **14**, 483 (2002).
[27]V. Gantmakher, Int. J. Mod. Phys. B **12** Nos. 29, 30 & 31 (1998); G. Sambandamurthy, L. W. Engel, A. Johansson, and D. Shahar, Phys. Rev. Lett. **92**, 107005 (2004); M. A. Steiner, G. Boebinger, and A. Kapitulnik, *ibid.* **94**, 107008 (2005); T. I. Baturina, A. Bilušić, A. Yu. Mironov, V. M. Vinokur, M. R. Baklanov, and C. Strunk, Physica C **468**, 316 (2008).
[28]S. Poran, E. Shimshoni, and A. Frydman, Phys. Rev. B **84**, 014529 (2011).
[29]D. Sherman, G. Kopnov, D. Shahar, and A. Frydman, Phys. Rev. Lett. **108**, 177006 (2012).
[30]Benjamin Sacépé, Thomas Dubouchet, Claude Chapelier, Marc Sanquer, Maoz Ovadia, Dan Shahar, Mikhail Feigel'man, and Lev Ioffe, Nat. Phys. **7**, 239 (2011).
[31]C. Chapelier, W. Escoffier, B. Sacépé, J. C. Villégier, and M. Sanquer, AIP Conf. Proc. **850**, 975 (2005).
[32]T. I. Baturina, A. Yu. Mironov, V. M. Vinokur, M. R. Baklanov, and C. Strunk, Phys. Rev. Lett. **99**, 257003 (2007).
[33]Madhavi Chand, Garima Saraswat, Anand Kamlapure, Mintu Mondal, Sanjeev Kumar, John Jesudasan, Vivas Bagwe, Lara Benfatto, Vikram Tripathi, and Pratap Raychaudhuri, Phys. Rev. B **85**, 014508 (2012).
[34]Signs of emergent granularity were observed in the magnetic-field tuned superconductor to insulator transition of thin layers of a-Pb by: J. S. Parker, D. E. Read, A. Kumar, and P. Xiong, Europhys. Lett. **75**, 950 (2006).
[35]M. D. Stewart Jr., Aijun Yin, J. M. Xu, and James M. Valles Jr., Science **318**, 1273 (2007).
[36]B. I. Shklovskii and A. L. Efros, *Electronic Properties of Doped Semiconductors* (Springer-Verlag, Berlin, Heidelberg, New-York, Tokyo, 1984); A. Frydman, O. Cohen, and Z. Ovadyahu, Solid State Commun. **83**, 249 (1992).
[37]A. Vaknin, A. Frydman, and Z. Ovadyahu, Phys. Rev. B **61**, 13037 (2000) and references therein.